Constraints on flat cosmologies with tracking quintessence from cosmic microwave background observations

Carlo Baccigalupi,[1,*] Amedeo Balbi,[2,†] Sabino Matarrese,[3,‡] Francesca Perrotta,[1,4,§] and Nicola Vittorio[2,‖]
[1]*SISSA/ISAS, Via Beirut 4, 34014 Trieste, Italy*
[2]*Dipartimento di Fisica, Università di Roma "Tor Vergata," and INFN, Sezione di Roma II via della Ricerca Scientifica 1, 00133 Roma, Italy*
[3]*Dipartimento di Fisica "Galileo Galilei," Università di Padova, and INFN, Sezione di Padova via Marzolo 8, 35131 Padova, Italy*
[4]*Osservatorio Astronomico di Padova, Vicolo dell'Osservatorio 5, 35122 Padova, Italy*
(Received 6 September 2001; published 5 March 2002)

We constrain cosmological parameters in flat cosmologies with tracking dark energy (or quintessence) using the existing data on cosmic microwave background (CMB) anisotropies. We perform a maximum likelihood analysis using combined data from COBE-DMR, BOOMERanG, DASI and MAXIMA, obtaining estimates for the dark energy density Ω_Q and equation of state w_Q, the physical baryon density $\Omega_b h^2$, the scalar perturbation spectral index n_S, the ratio R between the tensor and scalar perturbation amplitude (or the tensor spectral index n_T). Dark energy is found to be the dominant cosmological component $\Omega_Q = 0.71^{+0.05}_{-0.04}$, with an equation of state $w_Q = -0.82^{+0.14}_{-0.11}$ (68% C.L.). Our best fit value of the physical baryon density is in good agreement with the primordial nucleosynthesis bound. We find no significant evidence for deviations from scale invariance, although a scalar spectral index slightly smaller than unity is marginally preferred. Finally, we find that the contribution of cosmological gravitational waves is negligible. These results confirm that quintessence is slightly preferred with respect to ordinary cosmological constant by the present CMB data.

DOI: 10.1103/PhysRevD.65.063520 PACS number(s): 98.80.Cq

I. INTRODUCTION

Accurate measurements of the cosmic microwave background (CMB) anisotropy on subdegree angular scales represent one of the greatest achievements in modern cosmology. Two balloon-borne experiments BOOMERanG [1], MAXIMA [2], and the ground-based interferometer DASI [3] provided data on the CMB anisotropy angular power spectrum at multipoles corresponding to angular scales extending far below the degree, up to a few arcminutes. These results give statistically strong evidence for one peak in the power spectrum on angular scales corresponding to a degree in the sky and significant indications for a second and a third peak on smaller angles, confirming and extending earlier and less accurate data from BOOMERanG and MAXIMA [4], Together with the plateau observed by the Cosmic Background Explorer (COBE) Differential Microwave Radiometer (DMR) [5] on larger angular scales, these CMB data favor a flat Friedmann-Robertson-Walker (FRW) cosmological model and strongly support the existence of superhorizon, almost scale-invariant curvature perturbations at decoupling, which oscillate coherently after horizon crossing; this is consistent with a primordial phase of accelerated expansion as predicted in the context of the simplest inflationary cosmology [6].

The CMB anisotropy is strongly sensitive to the amount of baryons in the universe, especially through the relative amplitude of acoustic peaks. Measurements of the physical baryon density $\Omega_b h^2$ from the CMB (where Ω_b is the ratio of baryons to critical density today, and h is the present Hubble parameter H_0 in units of 100 km/sec/Mpc) are consistent with the big bang nucleosynthesis (BBN) [7]. This indicates that baryons can only account for roughly 5% of the critical density. In fact, several pieces of evidence, including CMB anisotropy measurements, suggest that the bulk of the total energy density is in some form of "dark" nonbaryonic component, with cold dark matter particles (CDM) contributing roughly 25% of the critical density, while about 70% of the total energy density is made of a smooth component with negative equation of state. The latter, which is the subject of the present work, and is described in detail below, has attracted a lot of interest in recent years and is commonly known as "dark energy" or "quintessence."

There are at least three independent pieces of evidence in favor of dark energy. First, type Ia supernovae observations indicate that the universe is experiencing a phase of accelerated expansion [8,9]; recently it has been also noticed that acceleration is a relatively recent occurrence in the cosmological evolution [10]. In FRW cosmologies, cosmic acceleration is possible only if a component with equation of state less than $-1/3$ is dominating the expansion. Second, best fits of the present CMB data favor a total energy density which is very close to the critical value [1–3]. Third, large scale structure observations suggest a universe with a low density of clustered material [11].

On the theoretical side, justifying the observed amount of vacuum energy is extremely difficult. Without entering in a detailed discussion of the cosmological constant problem, which is probably the greatest mystery in modern fundamen-

*Email address: bacci@sissa.it
†Email address: balbi@roma2.infn.it
‡Email address: matarrese@pd.infn.it
§Email address: perrotta@sissa.it
‖Email address: vittorio@roma2.infn.it

tal physics [12], we mention here the main aspects of this difficulty. If one tries to interpret it as a vacuum expectation value of some fundamental quantum field, any known scale of particle physics is tens of order of magnitude larger than the observed one, up to 120 orders of magnitude in the case of the Planck scale, leading to an evident ''fine-tuning'' problem. Moreover, this extremely low level of vacuum energy is such that it is dominating the cosmic expansion right now, leading to a ''coincidence'' or ''why now'' problem. The interest toward dark energy or quintessence models, first introduced in [13,14], resides in their potential ability to alleviate these fine-tuning problems, at least at classical level. Quintessence is the simplest generalization of the cosmological constant, involving a scalar field ϕ with potential V, which provides the required amount of vacuum energy today. Scenarios with inverse power-law potentials [13,15], interestingly connected with high energy particle physics models [16], have been proven to admit the existence of ''tracking'' solutions in which the dark energy is able to reach the required value today starting from a very wide set of initial conditions in the remote past, thus removing the previously mentioned fine-tuning problem [13,17], at least for what concerns cosmological classical trajectories. Scenarios with exponential potentials [14,15], suggested by string theories [18], have been demonstrated to possess ''scaling'' solutions in which the scalar field energy density scales as the dominant cosmological component, either matter or radiation. Recently, extended quintessence models [19], in which the dark energy possesses an explicit coupling with the Ricci scalar, have been studied [20–23]; a detailed study of tracking trajectories and of their effects on CMB and Large Scale Structure can be found in Ref. [24]. In the next section we briefly recall how a quintessence component induces its main effects on CMB spectra.

It is therefore interesting to study how the measured CMB anisotropy constrains quintessence models. This has been done in several ways in the past, by considering earlier data from MAXIMA and BOOMERanG [4]. CMB anisotropies in (extended) quintessence models have been extensively studied in [19,24], where the CMBFAST [31] code for the computation of cosmological perturbations was upgraded to include scalar-tensor theories of gravity, both for the background and the perturbations, in full generality. In a previous work by us [25], a minimally coupled quintessence with inverse power law potentials in the tracking regime, was assumed, to obtain constraints on the quintessence energy density and its equation of state: we found $0.3 \lesssim \Omega_Q \lesssim 0.7$ and $-1 \lesssim w_Q \lesssim -0.6$ at 95% confidence level, favoring potentials $V(\phi) \propto \phi^{-\alpha}$ with $\alpha \lesssim 2$. In Ref. [26], limits on the coupling between quintessence and dark matter have been obtained. In [27] constraints from exponential and inverse power law potentials have been compared. More recently [28–30] the impact on CMB anisotropies of the spectral separation of acoustic peaks has been studied.

In this work we consider the most recent data from BOOMERanG, MAXIMA, and DASI, and we relax many of the assumptions made in [25] on the underlying cosmological model, deriving constraints not only on the quintessence parameters but also on the abundance of cosmological gravitational waves, perturbation spectral indices, and physical baryon density $\Omega_b h^2$. We assume Gaussian and adiabatic initial conditions (see, however, Ref. [32]) and a flat geometry.

Before ending this section we wish to emphasize that our results on quintessence parameters have to be interpreted in a general way. In fact, as discussed in the next section, tracking solutions with inverse power law potentials predict a nearly constant equation of state at redshift where the quintessence is important: the latter case coincides with the simplest model of quintessence, where this is assumed to consist of a smooth component with constant $w_Q \geqslant -1$, independently of its nature. Therefore, before going to the specific potential parameters, our results on w_Q constrain the time variation of the vacuum energy from a general point of view.

The paper is organized as follows. In Sec. II we briefly review the theoretical properties of cosmologies with dark energy. In Sec. III we describe the region in parameter space which we investigate. In Sec. IV we show the results of the likelihood analysis of CMB data. Section V contains a discussion of our results.

II. TRACKING QUINTESSENCE AND CMB ANISOTROPIES

In this section we review the relevant aspects of tracking quintessence scenarios, highlighting the scalar field dynamics and the main effects on CMB anisotropies. We use our numerical code which is a modified version of CMBFAST [31], integrating scalar field cosmological equations for background dynamics as well as linear perturbations, in the general context of scalar-tensor theories of gravity, see [19,24] for details.

We restrict our analysis to minimally coupled quintessence. By considering the conformal time τ in a FRW metric, the Fridemann and Klein-Gordon equations for the evolution of the scale factor a and for the dark energy field ϕ take the form

$$\mathcal{H}^2 = \left(\frac{\dot{a}}{a}\right)^2 = \frac{8\pi G}{3}\left(a^2 \rho_{fluid} + \frac{1}{2}\dot{\phi}^2 + a^2 V\right),$$

$$\ddot{\phi} + 2\mathcal{H}\dot{\phi} = -a^2 V_\phi, \tag{1}$$

where the dot and the subscript ϕ denote differentiation with respect to the conformal time τ and to the quintessence scalar field, respectively, while $fluid$ represents contributions from all the species but quintessence and $V(\phi)$ is the scalar field potential. We will generally describe the amount of a particular species x with the present-day ratio Ω_x of its energy density ρ_x to the critical one $\rho_c = 3(\mathcal{H}/a)^2/8\pi G$. As we already mentioned, several potential shapes are under study: cosine [33], exponential [16] and inverse power law [18]. The cosine type has been recently considered in the context of extended quintessence [34]. With an exponential type potential, dark energy possesses the same redshift dependence as the dominant component which is driving the cosmic expansion, either matter or radiation, and some *ad hoc* mechanism or a nontracking behavior is required in order to bring

it to domination. In the inverse power law case, the tracking solution possesses an approximately constant equation of state which is not set by the component which leads the cosmic expansion but by the potential exponent itself. We take therefore

$$V(\phi)=\frac{M^{4+\alpha}}{\phi^{\alpha}}, \tag{2}$$

where the value of $\alpha>0$ will be specified later and the mass-scale M is fixed by the level of energy contribution today from the quintessence field. As we did in our previous works [19,24,25], we integrate numerically Eqs. (1) with the potential (2) to get the evolution of cosmological background quantities. As first noted in [13], the quintessence scalar field joins tracking solutions, which are most simply expressed in terms of the quintessence energy density and pressure:

$$\rho_{\phi}=\rho_{\phi}^{kin}+\rho_{\phi}^{pot}=\frac{1}{2a^2}\dot{\phi}^2+V(\phi),$$

$$p_{\phi}=\rho_{\phi}^{kin}-\rho_{\phi}^{pot}. \tag{3}$$

We are interested in quintessence equations of state in the range $-1\leqslant w_Q\leqslant -0.5$, because this is the typical interval leading to cosmic acceleration today [8,9]; since during the tracking regime the equation of state is roughly constant in time, it follows that the quintessence energy density plays a role in the cosmic evolution only at low redshifts, $1+z\lesssim 10$, since the pressureless matter density increases much more rapidly with redshift. To give an intuitive description of the principal cosmological effects of quintessence, it is enough to describe tracking dynamics in the matter dominated era (MDE). Since during the MDE the scale factor goes as $a(\tau)\sim\tau^2$, it easy to see that a power law solution $\phi\propto\tau^{\gamma}$ to the Klein-Gordon equation (1) exists for

$$\alpha=\frac{6}{\gamma}-2. \tag{4}$$

In this regime, the quintessence energy density scales with redshift as

$$\rho_{\phi}\propto(1+z)^{3(1+w_Q)}, \tag{5}$$

where its equation of state is

$$w_Q=-\frac{2}{\alpha+2}. \tag{6}$$

Our numerical integrations reproduce with good approximation the tracking conditions (5), (6), even if the equation of state is not perfectly constant and this has interesting consequences [35]. The interesting feature of these solutions, which makes their importance as tracking trajectories, is that they can be reached starting from a very wide set of initial conditions, so that the initial dark energy density deep in the radiation dominated era (RDE) could have been between the present value and tens of orders of magnitude higher [17]. We show an example of this phenomenology in Fig. 1. In the top panel we plot the redshift evolution of matter, radiation and quintessence starting from different initial conditions for the model specified below in Eq. (14). Matter and radiation (light dotted curves) have the known scalings; quintessence trajectories converge to the same tracking regime starting from different initial conditions. The potential parameter is $M\simeq 0.6M_P$, where $M_P=1/\sqrt{G}$ is the Planck mass, and $\alpha=-0.8$; the initial conditions for the solid, short dashed and dashed curve respectively are

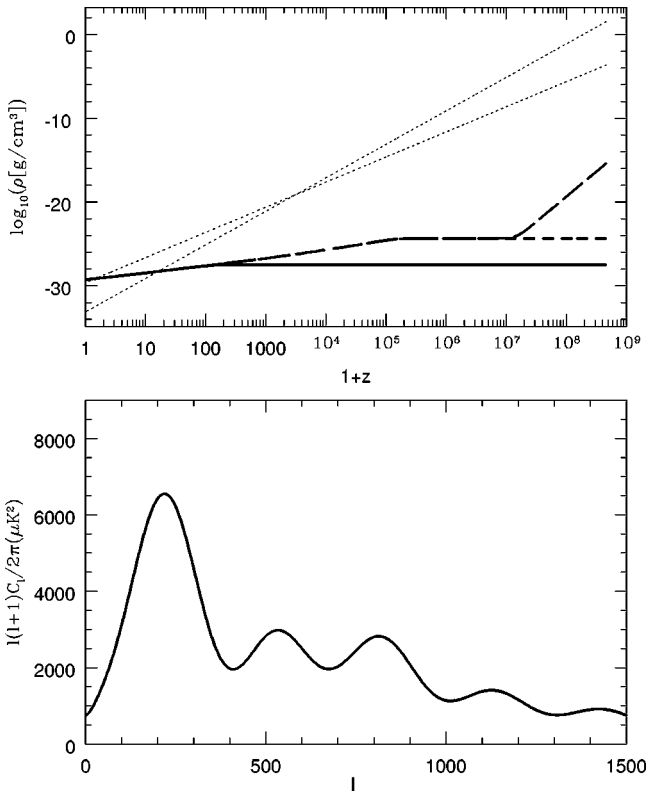

FIG. 1. Top panel: different quintessence trajectories converging to the same tracking regime (solid, long and short dashed curves); matter and radiation are represented by the dotted curves. Bottom panel: CMB spectra, nearly identical, for the three trajectories.

$$\phi_{in}=10^{-3}M_P,\ \ \rho_{in}^{kin}=0,$$

$$\phi_{in}=10^{-7}M_P,\ \ \rho_{in}^{kin}=0,$$

$$\phi_{in}=10^{-7}M_P,\ \ \rho_{in}^{kin}/\rho_{in}^{pot}=10^9. \tag{7}$$

These examples give an idea of the stability of tracking solutions. Since the different trajectories differ only at high redshifts when quintessence is subdominant the corresponding CMB spectra, shown in the bottom panel, are to high precision indistinguishable.

Cosmological linear perturbations, including quintessence fluctuations $\delta\phi$ obeying the perturbed Klein-Gordon equation

$$\delta(\Box\phi)+V_{\phi\phi}\delta\phi=0, \tag{8}$$

are numerically evolved starting from Gaussian adiabatic initial conditions: we refer to our previous works [32,19,24] for full details and formalism. Here we give only an intuitive description of the main effects of quintessence on CMB, which can be understood by considering the tracking behavior of the background evolution as expressed by Eqs. (5) and (6). Note that the tracking regime itself is strictly valid only if matter dominates the expansion. When quintessence comes to dominance the universe accelerates its expansion and the dark energy leaves the tracking regime. This makes the present equation of state different from the one during the tracking regime; however, this difference is only at the level of 10% for all the cases we consider in deriving our constraints.

As w_Q moves from the cosmological constant case (-1) to larger values, the conformal distance τ_{dec} to the last scattering surface gets reduced:

$$\tau_{dec}=H_0^{-1}\int_0^{z_{dec}}\frac{dz}{\sqrt{\Omega_{matter}(1+z)^3+\Omega_Q(1+z)^{3(1+w_Q)}}}. \tag{9}$$

As a consequence, the location of all the acoustic features in the CMB spectra shifts toward lower multipoles, corresponding to large angular scales in the sky.

The same mechanism leads to a reduction of the integrated Sachs-Wolfe (ISW) effect. The latter is represented by extra power at low multipoles, $l\lesssim 10$, caused by the dynamics of gravitational potentials at low redshift, $z\lesssim 10$ [37]; since the distance decreases in quintessence models with respect to cosmological constant ones, as shown by Eq. (9), the gravitational potentials dynamics is reduced correspondingly. However, for values of w_Q well above -1, the quintessence starts to dominate the cosmic expansion earlier in time, leading to an enhancement of the time interval in which the cosmic equation of state changes and therefore to an increase of the ISW power. As a consequence of these two competing effects, the ISW effect gets slightly reduced for $-1\lesssim w_Q\lesssim -0.8$, while it increases for larger values.

These two effects are purely geometric, i.e., they do not affect, for a given level of Ω_Q, the shape of the acoustic peaks on subdegree angular scales. The latter changes if Ω_Q and the ratio between CDM and baryons changes.

In the next section we will discuss in detail the cosmological parameters that we consider, and the region in the parametric space which we investigate.

III. GRIDDING COSMOLOGICAL PARAMETERS

In this work we improve considerably the extension and the gridding of the cosmological parameter space with respect to what we did in Ref. [25].

We consider flat cosmologies and fix the value of the Hubble parameter at present to

$$H_0=65\ \ \text{km/sec/Mpc}, \tag{10}$$

in agreement with current estimates [36]. We then vary the present ratio of baryon to critical density, in order to obtain different values of the physical baryon density, $\Omega_b h^2$. The amount of baryons in the universe is one of the most important quantities which affect CMB acoustic oscillations. At decoupling, any photon-baryon density fluctuation at wave number k which is entering the horizon oscillates between compression and rarefaction under the effect of the potential wells and hills caused by the dark matter perturbations. Increasing the baryon amount favors compression with respect to rarefaction peaks, simply because it shifts toward the bottom of the potential wells the rest position of the oscillator [37]. As we already stressed, tracking quintessence is described by its energy density today and by its equation of state. The radiation component is made of photons and three massless neutrino families; the matter component is made of CDM plus baryons.

Concerning perturbations, we allow for departure from scale invariance of the initial perturbation spectrum, as well as for a nonzero amplitude of cosmological gravitational waves. Scale invariance is related to the scalar spectral index, n_S; the latter can be defined in terms of the scalar perturbation spectrum at the horizon crossing as

$$\mathcal{P}(k)\propto k^{n_S-1}. \tag{11}$$

In the following, we will refer to cases with n_S larger or smaller than 1 as ''blue'' and ''red'' spectra, respectively [39].

Cosmological gravitational waves are tensor perturbations of the metric. Their power is maximal on superhorizon scales, corresponding to $l\lesssim 200$ on the CMB angular power spectrum, making this multipole region the only one where this component is detectable. Its power can be parametrized in terms of the ratio R between the tensor and the scalar contributions to the CMB quadrupole; moreover, we adopt the single field inflationary consistent relation (see, e.g., Ref. [6]), linking the tensor spectral index to R. Summarizing, we define

$$R=\frac{C_2^{tensor}}{C_2^{scalar}},\quad n_T=-\frac{R}{6.8}, \tag{12}$$

where $n_T=0$ means here a scale invariant tensor power spectrum at horizon crossing. The presence of gravitational waves as well as the deviation from scale invariance can be

TABLE I. Cosmological parameters values.

Parameter	Minimum	Maximum	Step
Ω_Q	0.40	0.80	0.02
w_Q	-1.00	-0.60	0.03
$\Omega_b h^2$	0.20	0.40	0.02
Ω_{CDM}	$1-\Omega_Q$	$1-\Omega_Q$	0.02
n_S	0.90	1.10	0.02
R	0	0.50	0.05
n_T	$-R/6.8$	$-R/6.8$	0.05/6.8

related to the standard slow rolling parameters ϵ, η for single field inflation, which are defined in terms of the inflaton potential and its first two derivatives (see, e.g., Ref. [6]). One has

$$\epsilon = \frac{R}{13.6}, \quad \eta = \frac{1}{2}\left(n_S - 1 + \frac{3R}{6.8}\right). \tag{13}$$

A summary of the values of the cosmological parameters considered in this work is given in Table I.

IV. MEASURES FROM EXPERIMENTAL DATA

In this section we compare theoretical CMB angular power spectra corresponding to the models in Table I with the most recent data from BOOMERanG, MAXIMA and DASI, as published in [1–3], as well as with the 4 year COBE-DMR data [5]. Our data set consists of 65 data points: 19 from BOOMERanG in the range $76 \leqslant l \leqslant 1025$, 13 from MAXIMA in the range $36 \leqslant l \leqslant 1235$, 9 from DASI in the range $104 \leqslant l \leqslant 864$, and 24 from COBE-DMR in the range $2 \leqslant l \leqslant 25$. As in [25], for a given choice of parameters we compare the measured quantities $l(l+1)C_l/2\pi$ to their theoretical predictions by evaluating the likelihood of the data, $\mathcal{L} \propto \exp(-\chi^2/2)$. When possible (i.e., COBE and DASI), we use the offset-lognormal ansatz for the shape of the likelihood, as in [38]. We do not consider correlations among the data points of each experiment, as they are rather small [1–3]. We take into account the effect of each experiment calibration uncertainty (20%, 8% and 8% for BOOMERanG, MAXIMA and DASI, respectively [1–3]) on the measured power spectrum. We do not take into account beam and pointing inaccuracies, since the details of these uncertainties were not made publicly available by the teams. However, we believe these effects should not affect much the released data.

Likelihood curves for each parameter are shown in Fig. 2. Each curve is obtained by fixing all the other parameters to their best fit value. It is evident that the preferred flat cosmological model involves vacuum energy as the dominant component, at the 70% level. Moreover, our best fit value of the baryon density, $\Omega_b h^2 = 0.022$, is in good agreement with the primordial nucleosynthesis bounds, $\Omega_b h^2 = 0.020 \pm 0.002$ (95% C.L.) [7]. The primordial power spectrum is consistent with scale invariance, $n_S \simeq 1$, although slightly red spectra are favored. These results are in good agreement with previous analyses [1–3].

A first new result of our analysis is that models with a subdominant contribution of gravitational waves are favored. As we already stressed, the main effect of cosmological gravitational waves is to enhance the anisotropy power above the degree scale, at multipoles $l \lesssim 200$. The likelihood curves indicate that such a contribution is unlikely to be required by the present data. The relative height of the CMB acoustic peaks with respect to the plateau region is likely to be determined mainly by the other relevant parameters, i.e., the relative abundance of cosmological components, the Hubble parameter, the scalar spectral index.

However, for the purposes of this work the most important result is the preference for quintessence models over cosmological constant ones, as implied by a clear peak in the likelihood curve at $w_Q \simeq 0.8$. This result confirms and strengthens our previous findings [25]: a remarkably similar result, although with larger confidence regions, was obtained

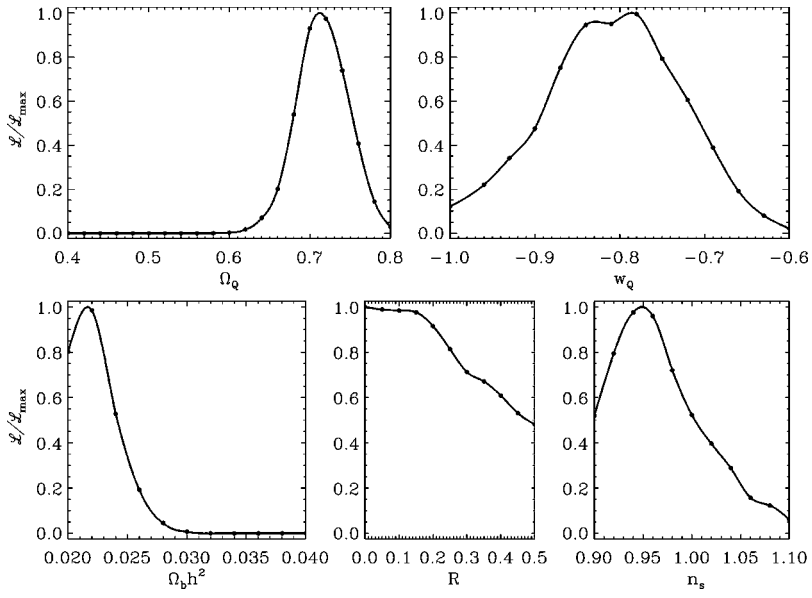

FIG. 2. Likelihood curves for cosmological parameters of Table I, normalized to the peak value.

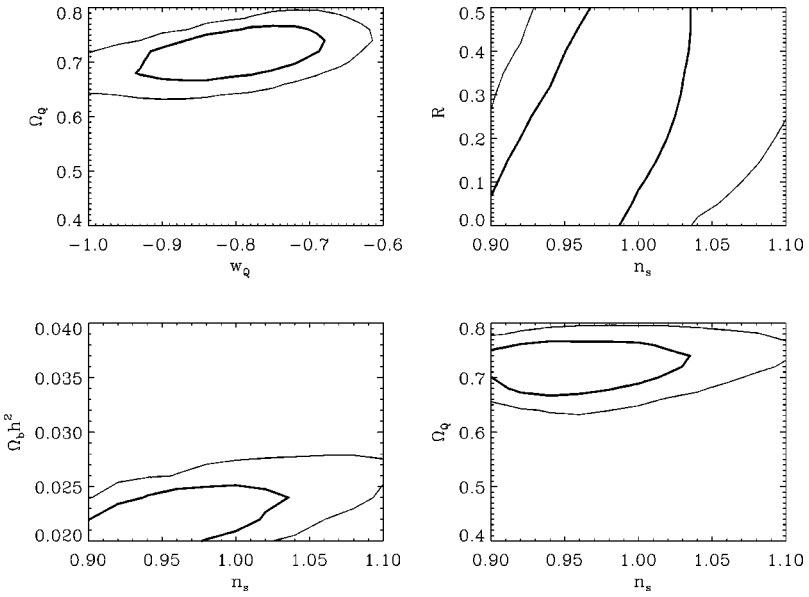

FIG. 3. Likelihood contours at 68% (heavy lines) and 95% (light lines) confidence levels.

by considering earlier CMB data release [4], as well as a reduced grid in number of parameters and gridding steps. Here we are obtaining almost the same measure of the vacuum energy equation of state, but considering the most recent data as well as allowing for variation of new parameters, namely the gravitational wave amplitude and the scalar spectral index. To understand the robustness of this result, it is natural to search what is the dominant effect of quintessence compared to the cosmological constant, directly on the CMB spectrum. We shall return to this point below.

Figure 3 shows confidence regions for different parameter combinations. Heavy and light lines represent 68% and 95% confidence levels, respectively. The highest degeneracy concerns the (R,n_s) plane. This degeneracy has a simple explanation. Increasing the scalar spectral index has the effect of enhancing the CMB peaks with respect to the region at $l \lesssim 200$, and this is disfavored by the data. The presence of a tensor component reintroduces power at low multipoles, so that its net effect, once the power spectrum is normalized, is to reduce the excess power of ''blue'' models at high l. The constraints in the (R,n_S) plane, in terms of the parameters ϵ and η defined in Eqs. (13), appear as in Fig. 4.

In all the other cases the contours are closed, at least at 68% confidence level. Summarizing, our best estimate of the cosmological parameters considered in this work are, at the 68% confidence level:

$$\Omega_Q = 0.71^{+0.05}_{-0.04}, \quad w_Q = -0.82^{+0.14}_{-0.11},$$

$$\Omega_b h^2 = 0.022 \pm 0.003, \quad n_S = 0.95 \pm 0.08,$$

$$R \lesssim 0.5 (n_T = -R/6.8). \tag{14}$$

We have fit 65 data points using approximately 9 parameters (5 cosmological parameters, 3 calibration parameters and an overall normalization of the power spectrum) so that the number of degrees of freedom (DOF) is roughly DOF $\simeq 65 - 9 = 56$. Our best fit has $\chi^2 = 57$, and $\chi^2/\mathrm{DOF} \simeq 1$. The best fit power spectrum, together with the experimental data, is shown in Fig. 5.

Before closing this section, let us translate our limits on the quintessence equation of state in terms of the potential slope α defined in Eq. (2). As we already stressed, the result (14) concerning the equation of state provides general evidence in favor of a time variation of the cosmological vacuum energy; the reason is that tracking trajectories with inverse power laws correspond to a nearly constant equation of state at the redshift of interest, which is the simplest model of quintessence. It is however interesting to determine the corresponding interval in the potential slope; tracking trajectories with a present equation of state as in Eq. (14) correspond to exponents

$$\alpha = 0.8^{+0.6}_{-0.5}. \tag{15}$$

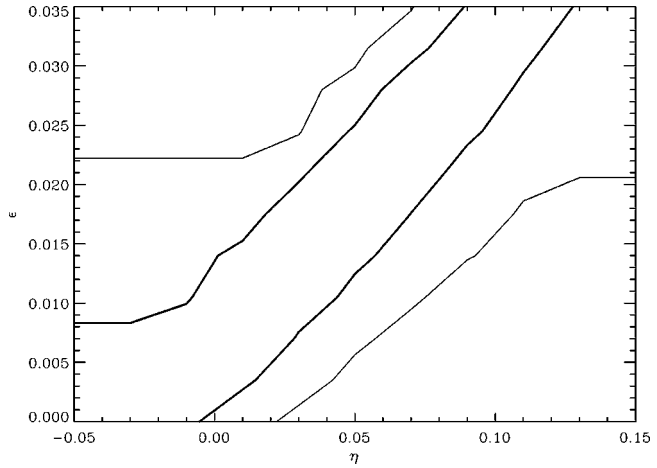

FIG. 4. Likelihood contours at 68% (heavy lines) and 95% (light lines) confidence levels in the plane of the inflationary slow rolling parameters ϵ, η defined in Eq. (13).

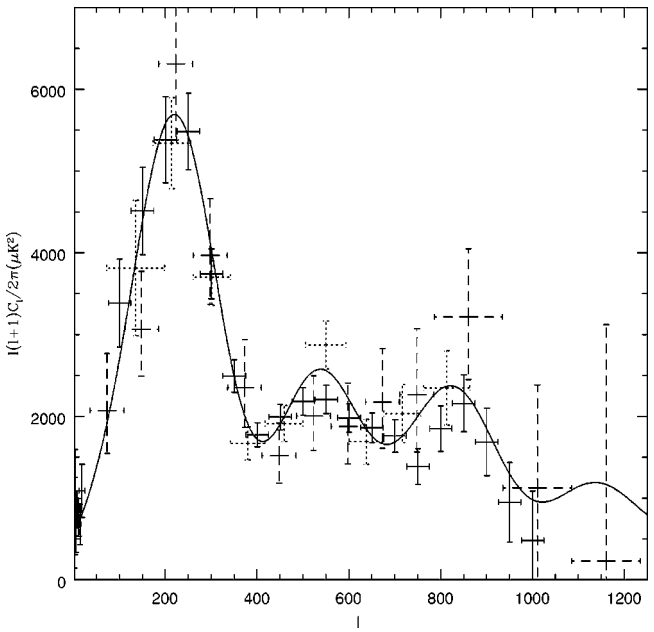

FIG. 5. Best fit cosmological model vs experimental data, $\Omega_Q = 0.72, w_Q = -0.8, \Omega_b h^2 = 0.022, n_s = 0.96, R = 0$. Solid error bars are for COBE (low multipoles) and BOOMERanG data, dashed and dotted for MAXIMA and DASI data, respectively.

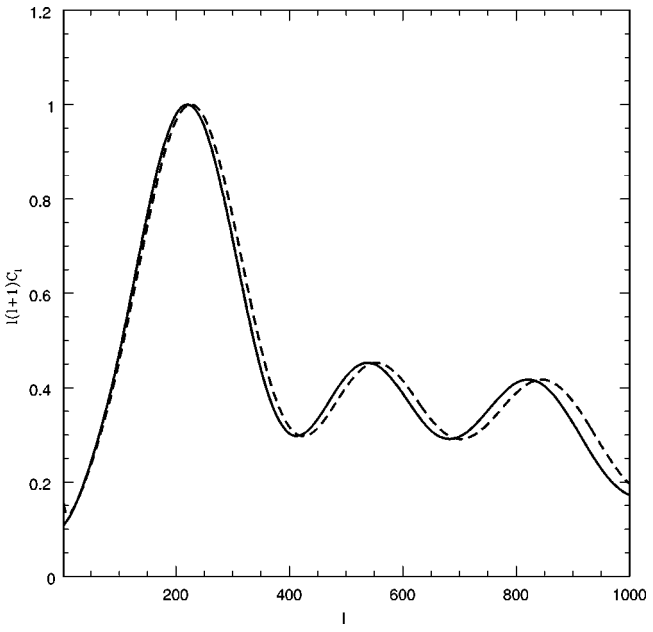

FIG. 6. First peak normalized CMB spectra for our best fit model ($w_Q = -0.8$, solid line) and its cosmological constant equivalent ($w_Q = -1$, dashed line).

Note that this is slightly different, although within a 1σ interval, from what would be obtained from Eq. (6), $\alpha = 0.7^{+0.2}_{-0.5}$. As we already mentioned, this is because the result (15) is numerically obtained from the present equation of state, which is slightly different from its value during the tracking regime.

This completes the constraints obtained from the comparison of our CMB spectra with the data. The most interesting aspect is the evidence in favor of a time variation of the vacuum energy component. In the next section we will discuss the robustness of these results.

V. DISCUSSION

Our results (14) have been obtained under a number of assumptions.

First, all the perturbations, including those in the quintessence component, are assumed to be Gaussian and initially perfectly adiabatic [32]. The tensor spectral index has been related to the amplitude of gravitational waves through the consistency relation (12); moreover, the global geometry is assumed to be flat. Even if these choices reduce considerably the parameter space region that we explore, they are justified by the prediction of the simplest inflationary models [6]. In addition, we assumed three massless neutrino families as well as a dark matter type which is purely cold; these conditions are those currently preferred by data on the large scale structure of the Universe [11].

Within these hypotheses, our comparison with CMB data revealed an interesting indication in favor of a time-varying vacuum energy. Even if this result depends crucially on the present CMB data which are still far from the performances that will be reached by satellite measurements [40,41], two questions arise. First, which is the effect of quintessence, compared with a pure cosmological constant, which makes present data prefer a quintessence component. Second, which cosmological parameter not considered in this work can mimic the effects of quintessence, thus undermining the robustness of our results.

We address the first question by comparing the CMB spectrum which represents the best fit (14) with its cosmological constant analog, in which all the parameters have the same value except for the equation of state, which is set to -1. The two spectra are compared in Fig. 6, normalized to the first peak height. It is evident that they differ mainly because quintessence causes a systematic shift of all the acoustic features toward larger angular scales, or lower multipoles; as we already mentioned in Sec. II, this is due to a progressive reduction of the conformal distance between us and the last scattering surface, as w_Q moves from -1 to higher values. Note also that the effect is small compared to the data error bars; indeed the cosmological constant, at the 95% confidence level, is still compatible with present data, as it is evident in Figs. 2 and 3.

The answer to the second question can now be given. If we fix the relative abundances today, the only parameter which we do not consider and that could mimic the projection effect in Fig. 6 is the cosmic curvature, represented by the total density parameter Ω_{tot}. It is indeed well known that a closed universe with $\Omega_{tot} > 1$ moves the acoustic features of the CMB spectrum toward smaller multipoles [37]. This argument is supported by earlier constraints on cosmological parameters—obtained without considering quintessence models—that were set by experiments measuring subdegree CMB anisotropies; the quoted results for Ω_{tot} were $1.04^{+0.05}_{-0.05}$ (or $1.02^{+0.06}_{-0.05}$), $0.90^{+0.18}_{-0.16}$, 1.04 ± 0.06 for BOOMERanG, MAXIMA and DASI, respectively [1–3]. Al-

though flatness is well within 1σ for all the experiments, it is however interesting that quintessence offers a mechanism to explain the slight preference of the existing data for closed models, the same mechanism being the reason why we find indications in favor of a dynamical vacuum energy in this work.

We conclude that, in the framework of flat cosmologies, the preference in favor of quintessence from present CMB data is quite robust. Future satellite missions [40,41] will allow to further test this result.

ACKNOWLEDGMENTS

We used a modified version of CMBFAST [31]. We are grateful to Fabio Pasian and Claudio Vuerli for support in data storing. A.B. acknowledges fruitful discussions with Domenico Marinucci.

[1] C.B. Netterfield *et al.*, astro-ph/0104460; P. De Bernardis *et al.*, astro-ph/0105296.
[2] A.T. Lee *et al.*, Astrophys. J. Lett. **561**, L1 (2001); R. Stompor *et al.*, *ibid.* **561**, L7 (2001).
[3] N.W. Halverson *et al.*, astro-ph/0104489; C. Pryke *et al.*, astro-ph/0104490.
[4] S. Hanany *et al.*, Astrophys. J. Lett. **545**, L5 (2000); A. Balbi *et al.*, *ibid.* **545**, L1 (2000); P. De Bernardis *et al.*, Nature (London) **404**, 955 (2000); A. Lange *et al.*, Phys. Rev. D **63**, 042001 (2001).
[5] C. Bennett *et al.*, Astrophys. J. Lett. **464**, L1 (1996); K.M. Gorski, Astrophys. J., Suppl. Ser. **114**, 1 (1998).
[6] A. Liddle and D.H. Lyth, *Cosmological Inflation and Large Scale Structure* (Cambridge University Press, Cambridge, England, 2000).
[7] K.A. Olive, G. Steigman, and T.P. Walker, Phys. Rep. **333**, 389 (2000); S. Burles, K.M. Nollett, and M. Turner, Astrophys. J. Lett. **552**, L1 (2001).
[8] S. Perlmutter *et al.*, Astrophys. J. **517**, 565 (1999).
[9] A. Riess *et al.*, Astron. J. **116**, 1009 (1998).
[10] M.S. Turner and A. Riess, astro-ph/0106051; A.G. Riess *et al.*, Astrophys. J. **560**, 49 (2001).
[11] J.A. Peacock, Nature (London) **410**, 169 (2001).
[12] S.E. Rugh and H. Zinkernagel, hep-th/0012253.
[13] P.J.E. Peebles and B. Ratra, Astrophys. J. Lett. **325**, L17 (1988); B. Ratra and P.J.E. Peebles Phys. Rev. D **37**, 3406 (1988).
[14] C. Wetterich, Nucl. Phys. **B302**, 668 (1988).
[15] A.R. Liddle and R.J. Scherrer, Phys. Rev. D **59**, 023509 (1999).
[16] M. Gasperini, Phys. Rev. D **64**, 043510 (2001).
[17] P.J. Steinhardt, L. Wang, and I. Zlatev, Phys. Rev. D **59**, 123504 (1999).
[18] A. Masiero, M. Pietroni, and F. Rosati, Phys. Rev. D **61**, 023504 (2000).
[19] F. Perrotta, C. Baccigalupi, and S. Matarrese, Phys. Rev. D **61**, 023507 (2000).
[20] J.P. Uzan, Phys. Rev. D **59**, 123510 (1999).
[21] L. Amendola, Phys. Rev. D **60**, 043501 (1999).
[22] T. Chiba, Phys. Rev. D **60**, 083508 (1999).
[23] N. Bartolo and M. Pietroni, Phys. Rev. D **61**, 023518 (2000).
[24] C. Baccigalupi, S. Matarrese, and F. Perrotta, Phys. Rev. D **62**, 123510 (2000).
[25] A. Balbi, C. Baccigalupi, S. Matarrese, F. Perrotta, and N. Vittorio, Astrophys. J. Lett. **547**, L89 (2001).
[26] L. Amendola, Phys. Rev. Lett. **86**, 196 (2001).
[27] P. Brax, J. Martin, and A. Riazuelo, Phys. Rev. D **62**, 103505 (2000).
[28] M. Doran, M. Lilley, J. Schwindt, and C. Wetterich, Astrophys. J. **559**, 501 (2001).
[29] M. Doran, M. Lilley, J. Schwindt, and C. Wetterich, astro-ph/0105457.
[30] P.S. Corasaniti and E.J. Copeland, Phys. Rev. D **65**, 043004 (2002).
[31] U. Seljak and M. Zaldarriaga, Astrophys. J. **469**, 437 (1996).
[32] F. Perrotta and C. Baccigalupi, Phys. Rev. D **59**, 123508 (1999).
[33] K. Coble, S. Dodelson, and J. Friemann, Phys. Rev. D **55**, 1851 (1997).
[34] T. Chiba, Phys. Rev. D **64**, 103503 (2001).
[35] S. Podariu and B. Ratra, Astrophys. J. **532**, 109 (2000).
[36] M.C. Liu and J.R. Graham, Astrophys. J. Lett. **557**, L31 (2001); B.S. Mason, S.T. Meyers, and A.C.S. Readhead, *ibid.* **555**, L11 (2001); W.L. Freedman *et al.* Astrophys. J. **553**, 47 (2001).
[37] W. Hu, U. Seljak, M. White, and M. Zaldarriaga, Phys. Rev. D **57**, 3290 (1998).
[38] J.R. Bond, A.H. Jaffe, and L.E. Knox, Astrophys. J. **533**, 19 (2000).
[39] S. Mollerach, S. Matarrese, and F. Lucchin, Phys. Rev. D **50**, 4835 (1994).
[40] E.L. Wright, New Astron. Rev. **43**, 257 (1999).
[41] N. Mandolesi *et al.*, PLANCK Low Frequency Instrument, a proposal submitted to ESA, 1998; J.L. Puget *et al.*, High Frequency Instrument for the PLANCK mission, a proposal submitted to ESA, 1998.